Available online at www.sciencedirect.com

ScienceDirect

Procedia Structural Integrity 26 (2020) 155–165

Structural Integrity Procedia

www.elsevier.com/locate/procedia

The 1st Mediterranean Conference on Fracture and Structural Integrity, MedFract1

# Nano $CaCO_3$ particles in cement mortars towards developing a circular economy in the cement industry

Isabella Cosentino[a*], Freddy Liendo[b], Mara Arduino[b], Luciana Restuccia[a], Samir Bensaid[b], Fabio Deorsola[b], Giuseppe Andrea Ferro[a]

[a]*Department of Structural, Building and Geotechnical Engeneering, Politecnico di Torino, Corso Duca degli Abruzzi 24, Turin 10129, Italy*
[b]*Department of Applied Science and Technology – Politecnico di Torino, Corso Duca degli Abruzzi 24, Turin 10129, Italy*

**Abstract**

This paper calls into question the effects of incorporating nano calcium carbonate ($CaCO_3$) particles in cement mortars, as they are interesting additive materials already successfully tested as cement nanofiller. These nanoparticles could potentially be prepared through the carbonation route using $CO_2$ from combustion gases from the cement industry. This could enable a circular-economy approach for carbon capture and its re-use within the cement industry, in a sustainable and synergistic manner. In this study, part of the cement content was substituted with commercial nano $CaCO_3$ particles to investigate their effects on the flexural and compressive strength of the resulting cement mortars, after curing for 7 and 28 days. Decreasing the cement content could lead to a reduction in the carbon footprint of cement, which is responsible for approximately 8% of global carbon dioxide emissions. Preliminary results using synthesized $CaCO_3$ particles as nanofillers showed that, after 7 days of curing, mechanical properties of cement mortars improved. This indicates that hydration reaction was accelerated since $CaCO_3$ acts as seeding for this reaction. By contrast, after 28 days of curing, no major improvement was observed. A higher content of calcium carbonate nanoparticles may have reduced the filler effect of these particles due to aggregation phenomena. In the present work, the effects of commercial nano $CaCO_3$ particles on cement hydration were investigated. Mechanical tests showed promising results both after 7 and 28 days of curing. This could lead to the reduction of the carbon footprint of cement manufacturing and produce increasingly better performing building materials. Thus, the development of a circular economy in the cement industry could be achieved.



*Keywords:* calcium carbonate; nanoparticles; cement industry; carbon dioxide; circular economy.

* Corresponding author. Tel.: +39 0110904849
*E-mail address:* isabella.cosentino@polito.it


10.1016/j.prostr.2020.06.019

## 1. Introduction

Green House Gas (GHG) emissions generated by cement manufacturing are very high and are responsible for approximately 8% of global emissions of carbon dioxide ($CO_2$). $CO_2$ is emitted as a by-product of clinker production in which calcium carbonate ($CaCO_3$) is calcinated and converted to lime (CaO), the primary component of cement. $CO_2$ is also emitted during cement production by fossil fuel combustion. However, $CO_2$ from fossil fuels is specifically accounted for in emission estimates for fossil fuels process (Andrew (2018)). Environmental concerns thus require the industry to develop means of reducing its critical level of harmful emissions.

Great opportunities lie in the utilization of cements based on alternative compositions, binding-phases and green chemistry. Fly ash, blast-furnace slag, silica fume are the alternative supply options for cement. Calcium sulfoaluminate cement, magnesium oxide based cement, geo-polymers have been developed.

Promising low cost carbon-based materials were incorporated in cement composites (Restuccia et al. (2016)). Pyrolyzed particles from food waste were used as nano/micro inert aggregates in the cementitious composites (Restuccia et al. (2016)). A standardized biochar from pyrolyzed feedstock was also used in view of a possible industrial production of biochar cement-based composites (Cosentino et al. (2019)). Higher flexural strength, fracture energy and ductility values were recorded for specimens with the addition of pyrolyzed nano particles compared to the sample specimens.

Particle size plays a key role in completely changing concrete technology: the smaller the particle, the higher the improvement in terms of mechanical properties (Restuccia et al. (2018), Ferro et al. (2014), Ferro et al. (2015)). The nanoscale provides a very high SSA/V ratio, with a wider contact between the particles and the surrounding matrix. This means a better performance compared to conventional materials. Nanoparticles densify microstructure and the interfacial transition zone, thereby reducing permeability, hence increasing the durability of the composites (Sanchez et al. (2010), Shaikh et al. (2014)). Recent research on nanotechnology in concrete involve $SiO_2$ nanoparticles (Sobolev et al. (2009)), ferric oxide ($Fe_2O_3$) nanoparticles (Khoshakhlagh et al. (2012)), titanium oxide ($TiO_2$) nanoparticles (Daniyal et al. (2019)), $Al_2O_3$ nanoparticles (Nazari et al. (2010)), calcium carbonate ($CaCO_3$) nanoparticles (Hashim et al. (2018), Supit et al. (2014)).

To date, nano $CaCO_3$ is widely used in cementitious composites due to its benefits on their properties through physical effects e.g. filler effect and nucleation effect, and chemical effects. However, agglomeration phenomena of nano $CaCO_3$ can reduce its effects significantly (Cao et al. (2019)). Research proved that incorporating nano calcium carbonate in cementitious composites is not harmful to their mechanical properties. It also has a positive synergic effect on the early-age strength, the hydration process and the durability of cementitious composites (Camiletti et al. (2013)). Hence, a large amount of research has been conducted to make clear the effects of $CaCO_3$ on cement paste, cement mortar or concrete.

A possible solution to the environmental problem linked to the cement industry could be to capture the $CO_2$ present in flue gases and re-use it within the cement industry to develop a circular economy in cement manufacturing. $CO_2$ could be recycled in the cement industry to produce valuable chemicals e.g. cement additives and concrete nanofillers to improve cementitious product quality. Nearly zero $CO_2$ cementitious composites could be developed by adding a $CaCO_3$ nanofiller produced via innovative recovery systems of carbon dioxide in cement manufacturing (Cosentino et al. (2019)). Cosentino et al. (2019) obtained nanosized pure calcite particles by employing a packed bed reactor via a carbonation route. The $CaCO_3$ synthesis was carried out by reacting calcium oxide with carbon dioxide in an experimental setup. The synthesized nano $CaCO_3$ particles were added to the cementitious composites in different percentages according to the cement weight. Results showed that after 7 days of curing, the flexural and compressive strength improved by increasing $CaCO_3$ content even if the optimal additional percentage proved to be 2%. By contrast, after 28 days of curing, a decrease of mechanical properties occurred in specimens with the addition of $CaCO_3$ compared to sample specimens (Cosentino et al. (2019)). This suggests that the hydration process was accelerated since $CaCO_3$ acts as seeding for this reaction. On the other hand, a higher quantity of nano $CaCO_3$ particles may have abated the filler effect of the particles due to phenomena of aggregation.

The present study investigates the effects of incorporating commercial nano $CaCO_3$ particles in cement mortars. The characteristics of nanoparticles selected are comparable to the synthesized particles in terms of purity, crystal phase, particle size distribution and morphology. This work provides an in-depth study on their behaviour in the cement matrix and their effects on the cement hydration.

A large amount of research indicates that nanoparticles act as a nucleation site in the cement hydration, thus accelerating the hydration rate (Camiletti et al. (2013), McDonald et al. (2019), Shaikh et al. (2014), Supit et al. (2014)). The cement hydration concerns changes that occur when anhydrous cement or one of its constituent phases is mixed with water (H.F.W. Taylor, 1997). The main phases present in cement are tricalcium silicate ($C_3S$), dicalcium silicate ($C_2S$), tricalcium aluminate ($C_3A$) and tetra calcium aluminoferrite ($C_4AF$) (Marangu et al. (2019)). They react in accordance with the mechanism shown in Figure 1. The hydration of $C_3S$ and $C_2S$ generates calcium hydroxide (CH) and amorphous calcium silicate hydrate (CSH), with the properties of a rigid gel which gives strength to cement-based materials (H.F.W.Taylor (1997), Marangu et al. (2019)). The hydration of $C_3A$ produces calcium aluminate hydrate (CAH), while CH/$C_4AF$ hydration forms tetra calcium alumino-13-hydrate ($C_4AH_{13}$) and tetra calcium ferrite-13-hydrate ($C_4FH_{13}$). In addition, in blended cement, the generated CH reacts with active silica and alumina in presence of water to make further CSH and calcium aluminate hydrate (CAH) during the pozzolanic reaction as follows:

$$CH + S + H \rightarrow CSH \tag{1}$$

$$CH + A + H \rightarrow CAH \tag{2}$$

The transformation of anhydrous compounds into the corresponding hydrates is a complex reaction and is influenced by several factors e.g. the water/cement ratio (w/c) or the composition of the cement and aggregates. Atmospheric conditions are also relevant in this process, because they could be less favorable to reaction. $CO_2$ could react with the resulting C-S-H in the formation of $CaCO_3$ and anhydrous silica, which would reduce the hardness and strength of the cement composite. Hence, high humidity and free $CO_2$ atmosphere are suitable conditions for the process (H.F.W.Taylor (1997)).
Within the framework of these criteria, research in this area is attracting widespread interest due to the possible development of a circular economy in the cement industry. Nano $CaCO_3$ particles are additive materials with high potential for cementitious composites. They could be produced via an innovative $CO_2$ emissions recovery system in cement manufacturing. Results from mechanical tests so far have been very encouraging (Cosentino et al. (2019), Cosentino et al. (2019)).

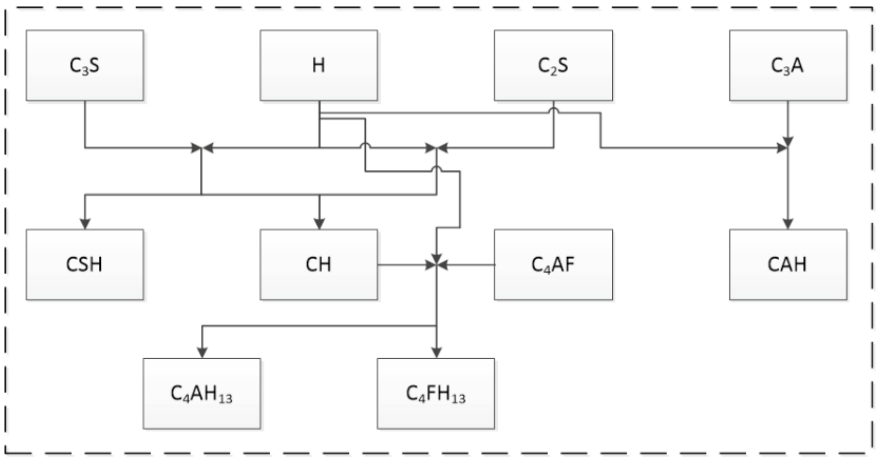


Fig. 1. The cement hydration mechanism scheme.

## 2. Materials and Methods

### *2.1. Materials*

Ordinary Portland Cement (Type II/A-LL, strength class 42.5 R) provided by Buzzi Unicem Group was used. It conforms to the harmonized European standard EN 197-1 and displays the CE marking as required by European

regulation 305/2011 (CPR). This cement may contain between 80-94% clinker and between 6-20% limestone. A maximum of 5% minor constituents is permitted (Table 1).

CEN Standard sand is pre-packed in bags with a content of (1350 ± 5) g that complies with the particle size distribution determined by sieve analysis on a representative sand sample of total mass not less than 1345 g, according to the European Standard EN 196-1 (Table 2).

Nano $CaCO_3$ particles were provided by Tec Star S.r.l with chemical and physical properties shown in Table 3.

Table 1. Physical/mechanical and chemical characteristics CEM II/A-LL 42.5 R Buzzi Unicem

| Parameters | | | |
|---|---|---|---|
| Blaine specific surface | $cm^2/g$ | 3100-4500 | EN 196/6 |
| Initial setting time | min | > 130 | EN 196/3 |
| Volume stability | min | ≤ 10 | EN 196/3 |
| Flow test | % | > 80 | UNI 7044 |
| Compressive strength after curing for 2 days | MPa | > 25,0 | EN 196/1 |
| Compressive strength after curing for 28 days | MPa | > 47,0 | EN 196/1 |

Table 2. Particle size distribution of the CEN Reference Sand.

| Sieve analysis | | | | | | | |
|---|---|---|---|---|---|---|---|
| Square mesh size | mm | 2.00 | 1.60 | 1.00 | 0.50 | 0.16 | 0.08 |
| Cumulative sieve residue | % | 0 | 7 ± 5 | 33± 5 | 67 ± 5 | 87 ± 5 | 99 ± 1 |

Table 3. Chemical and physical properties of nano$CaCO_3$ by Tec Star S.r.l.

| Parameters | | |
|---|---|---|
| Appearance (form; color) | - | powder; white |
| Average particle size (XRD) | nm | 60 |
| Crystal Phase (XRD) | - | calcite |
| Purity | % | ≥ 99 |
| Tap density | $g/cm^3$ | 0.777 |

## *2.2. Methods*

Cement mortars were prepared in accordance with the European Standard EN 196-1 “Methods of testing cement - Part 1: Determination of strength”. One part Ordinary Portland Cement (OPC), three parts CEN Standard sand and one-half part deionized water were used. Part of the OPC content was substituted with commercial nano $CaCO_3$ particles in different percentages according to cement weight. A quantity equal to 7% addition of nano $CaCO_3$ was also added to cement mortars. Cement mortars mixtures design is shown in Table 4.

$CaCO_3$ slurry samples were prepared by gradually adding a known amount of $CaCO_3$ to a 250 mL beaker containing a known amount of cold distilled water according to the mixture composition. The suspension was continuously mixed by means of ultrasonication using a VCX 750 Sonicator & 13mm Probe, with an 85% amplitude. The resulting solution and the cement were poured into a stainless steel bowl and the standard procedure was applied to prepare experimental specimens. As soon as the slurry and the cement were brought into contact, the mixer was started at low speed. After 30 s of mixing, the sand was added during the next 30 s. Then the mixer was switched to high speed and continued for an additional 30 s. The mixer was stopped for 90 s, and the mortar adhering to the wall of the bowl was removed. The mixing continued at high speed for another 60 s. The test specimens were made by introducing the first of two layers of mortar into each of the mould compartments, then compacted using 60 jolts of the jolting apparatus. The

second layer was introduced and compacted with a further 60 jolts. Specimens were stored in a humid atmosphere for 24 hours, and, once they were unpacked, they were immersed in water at (20.0 ±1.0) ° C for 7 and 28 days curing.

Table 4. Cement mortars mix design

| ID Mixture | OPC | CEN Standard Sand | Deionized Water | Nano $CaCO_3$ |
|---|---|---|---|---|
| Mortar | 450 g | 1350 g | 250 g | 0.0 g (0%)* |
| $CaCO_3$_1%subst. | 445.5 g | 1350 g | 250 g | 4.5 g (1%)* |
| $CaCO_3$_2%subst. | 441 g | 1350 g | 250 g | 9.0 g (2%)* |
| $CaCO_3$_3%subst. | 436.5 g | 1350 g | 250 g | 13.5 g (3%)* |
| $CaCO_3$_7%subst. | 418.5 g | 1350 g | 250 g | 31.5 g (7%)* |
| $CaCO_3$_7%addit. | 450 g | 1350 g | 250 g | 31.5 g (7%)* |

*percentages according to the cement weight

The commercial nano $CaCO_3$ was chemically and physically characterized. The $CaCO_3$ powder was dispersed in isopropanol by means of ultrasonic mixing to obtain a stable crystal suspension (Vergaro et al., 2015) and about 1 mL of sample was put into a disposable polystyrene cuvette and size distribution was measured by Dynamic Light Scattering (DLS) method using particles size analyzer (Malvern nano ZS model).

Morphological characterization of the $CaCO_3$ powder was obtained using scanning and transmission electron microscopy (ZEISS MERLIN FE-SEM operated at 3 kV). Field Emission Scanning Electron Microscopy (FESEM) provides topographical at magnifications up to 1 000 000x and gives clear images resolutions down to 1 nm. The sample was prepared suspending a small quantity of nanoparticles in isopropanol, through ultrasonic mixing for 30 min, and subsequently placing a drop of the dispersion on a copper grid coated with a layer of amorphous carbon, and finally the sample was dried at room temperature before FESEM analysis.

Fragments of tested specimens were grinded to prepare the composite powder for the X-Ray Diffraction (XRD) analysis (Panalytical X'Pert Pro). The commercial nano $CaCO_3$ was also analysed through this technique. The different phases of the samples were examined in the 2θ range of 5-70° with a scanning step of 0.013° and a radiation CuKα, k= 1.54056 Å. The crystalline phase was identified by employing the Powder Diffraction File PDF-4/Minerals 2020 of JCPDS.

Thermogravimetric analysis was carried out on tested specimens with a TGA instrument Mettler Toledo 1600. TGA simultaneously measures the weight loss due to the decomposition of phases. About 50 mg of samples were heated from 25 °C to 800 °C with a constant heating ramp of 10 °C/min. The air was supplied with a constant flow rate (50 mL/min).

## 3. Mechanical test activity

Mechanical test activity was carried out on each experimental specimen in compliance with the European Standard EN 196-1, after 7 and 28 days of curing. Three Point Bending test (TPB) with a Zwick Line-Z050 testing machine with a load cell of 50 kN was performed on each experimental specimen. The load was increased at the rate of 50 N/s until failure. The span adopted was 100 mm. Flexural strength, $R_f$, in megapascals, was calculated by Equation 3:

$$R_f = \frac{1.5 * F_t * l}{b^3} \quad [MPa] \tag{3}$$

in which $F_t$ represents the load applied to the middle of the prism at fracture, in newtons; $l$ is the distance between the supports, in millimeters; $b$ is the side of the square section of the prism, in millimeters.

Compression test was performed on halves of the prism broken during TPB tests using a Zwick Roell SMART.PRO testing machine with a load cell of 1000 kN. The load was increased at the rate of 2400 N/s over the entire load application until failure. Compressive strength, $R_c$, in megapascals, was calculated by Equation 4:

$$R_c = \frac{F_C}{A} \ [MPa] \tag{4}$$

in which $F_c$ represents the maximum load at fracture, in newtons; $A$ is the area of the platens in square millimetres.

## 4. Results and discussion

Figure 2 shows the characterization of the commercial nano $CaCO_3$ particles. The XRD spectra (Figure 2a) was compared to pure $CaCO_3$ polymorph patterns in reference database and literature (Zhou et al. (2004)). The diffraction peaks are well consistent with pure calcite crystals and no presence of other crystalline phases, like metastable aragonite or vaterite, was determined. Calcite is the most stable crystalline phase of $CaCO_3$ in water (Rodriguez-Blanco et al. (2011), Kawano et al. (2009), Chen et al. (1997)) that means that it will not suffer any transformation once dispersed in water (Kawano et al. (2009)). It is also easier to study, control and improve their filler effect (d'Amora et al. (2020)). Therefore, the effect observed in these tests is due to the addition of calcite particles with a narrow particle size distribution with a mean particle size equal to 200 nm according to Figure 2b. Figures c-d show FESEM micrographs of these particles. Cubic primary nanoparticles with a size equal to 60 nm are appreciable. Distribution particle size (Figure 2b) shows higher sizes than the primary nanoparticles, probably because the measurement through DLS analysis allows the determination of the size of the aggregates formed by the cubic nanoparticles. Nevertheless, the FESEM analysis is in good agreement with the XRD spectra, since they present the classical cubic morphology of calcite (Chen et al. (1997), Rodriguez-Blanco et al. (2011), Kawano et al. (2009), Declet et al. (2016)).

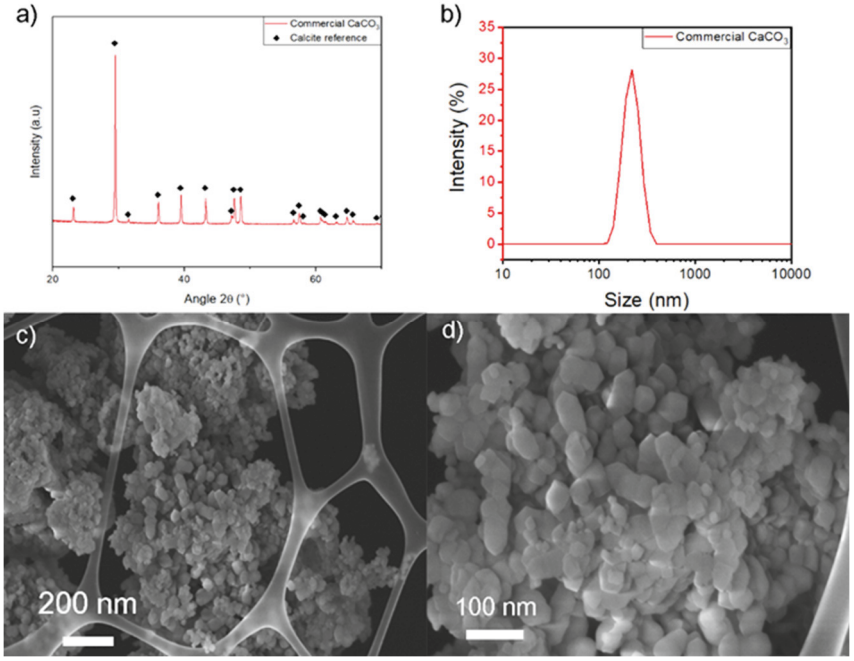


Fig. 2. $CaCO_3$ particles characterization. (a) X-Ray Diffraction; (b) Particle size Distribution; (c) (d) FESEM micrographs.

Figures 3a and 3b provide results from mechanical testing on all the experimental specimens. The flexural strength (Figure 3a) rose with the substitution of nano $CaCO_3$ after 7 and 28 days of curing. After 7 days of curing, this improvement was major. There was a 2.4% raise with 1% substitution, 5.3% raise with 2% substitution, 1.4% with 3% substitution, 5.8% with 7% substitution. After 28 days of curing, only in the case of 7% substitution of $CaCO_3$ there was 5.6% decrease of the flexural strength in specimens tested.

With regard to the compressive strength (Figure 3b), the lowest substitution percentages (1%, 2%) of nano $CaCO_3$ supplied good results in compression strength of specimens after 7 and 28 days of curing. On the other hand, the highest substitution percentages of nano $CaCO_3$ showed poor performance in compression tests but the 7% substitution of nano $CaCO_3$ provided an improvement of compressive strength after 7 days of curing. Obviously, these are preliminary results. Further mechanical tests are still needed to confirm this trend.

Different performance of cement mortars depending on 7% addition or 7% substitution of nano $CaCO_3$ is shown in Figure 4. Nano $CaCO_3$ added to cement mortars provided better results in terms of flexural and compressive strength compared to calcium carbonate substituted with the cement content.

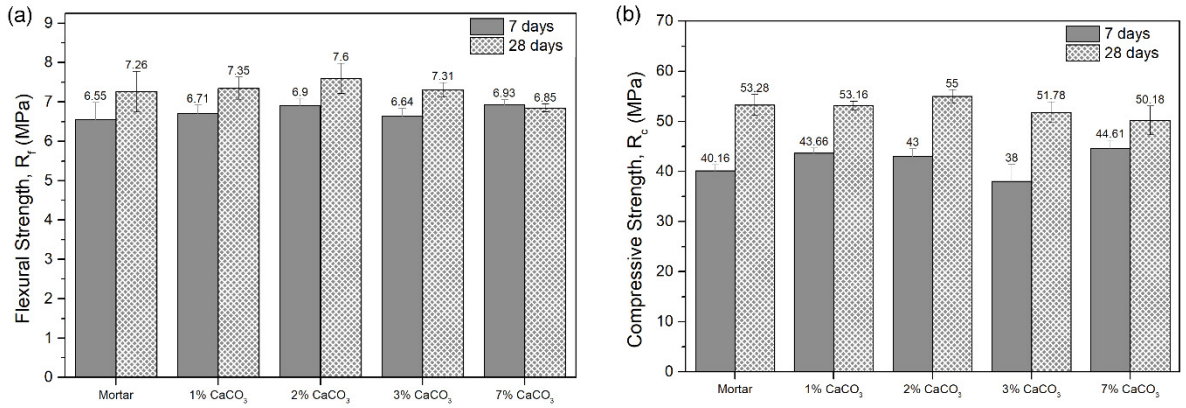


Fig. 3. Cement mortars with nano $CaCO_3$ substitued with part of cement: (a) Flexural strength (mean value) after 7 and 28 days of curing. (b) Compressive strength (mean value) after 7 and 28 days of curing.

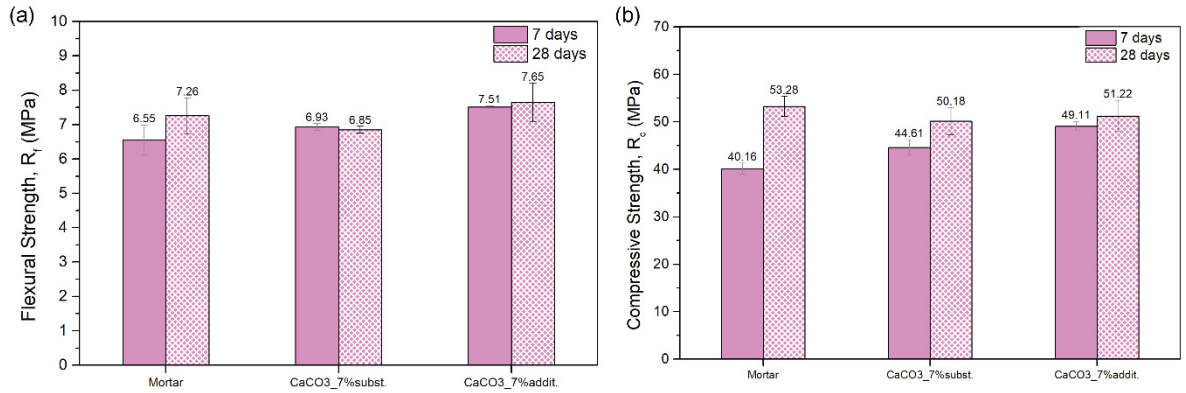


Fig. 4. Comparison 7% subst. - 7% addit. of nano $CaCO_3$. (a) Flexural strength (mean value) after 7 and 28 days; (b) Compressive strength (mean value) after 7 and 28 days.

Figures 5a and 5b present the TGA curves of the cement mortar specimens after curing for 7 and 28 days respectively. These curves describe the characteristic shape of hydrated cements (Gabrovšek et al. (2006)). According to the differential thermal analysis curve, mass loss before the 100 °C to 125 °C interval corresponds mainly to the water loss from moisture over cement surface, CSH gel and from dehydration of ettringite (AFt). Then, around 145 °C, there is the peak corresponding to monosulfate (AFm). Calcium hydroxide (CH) degrades at 440 °C, while the last mass losses between 550 and 725 °C can be attributed to OH-groups, carbonated phases from CSH gel and $CaCO_3$.

The advancement of the hydration of the cement is highlighted in Figure 6. The peak corresponding to CH is broader for specimens cured for 7 days compared to specimens cured for 28 days, which is shifted to the right because of the transformation of portlandite in more crystallized forms (Gabrovšek et al. (2006)). These peaks also have a lower area, which indicates that CH reacts with $C_2AF$ to form $C_4AH_{13}$ and $C_4FH_{13}$ according to the mechanism shown in Figure 1. Moreover, the peaks of structured OH- and carbonated phases after 28 days of curing are shifted to higher temperatures with respect to after 7 days of curing for both cases, cement mortars containing 1% and 2% substutition of nano $CaCO_3$. This indicates an ordering improvement of the CSH gel structure after the longer hydration time and higher crystallization of carbonated phases (Gabrovšek et al. (2006)). Quantifying the content of AFt, AFm and CSH is quite difficult due to the peaks overlapping. On the other hand, the content of calcium hydroxide (CH(%)) can be estimated according to the Taylor equation (Equation 5) (H.F.W.Taylor (1997), Shaikh et al. (2014)).

$$CH\ (\%) = WL_{CH}(\%)\frac{MW_{CH}}{MW_w} \tag{5}$$

where, $WL_{CH}(\%)$ is the CH weight loss percentage, $MW_{CH}$ and $MW_w$ are the CH and water molar weights respectively.

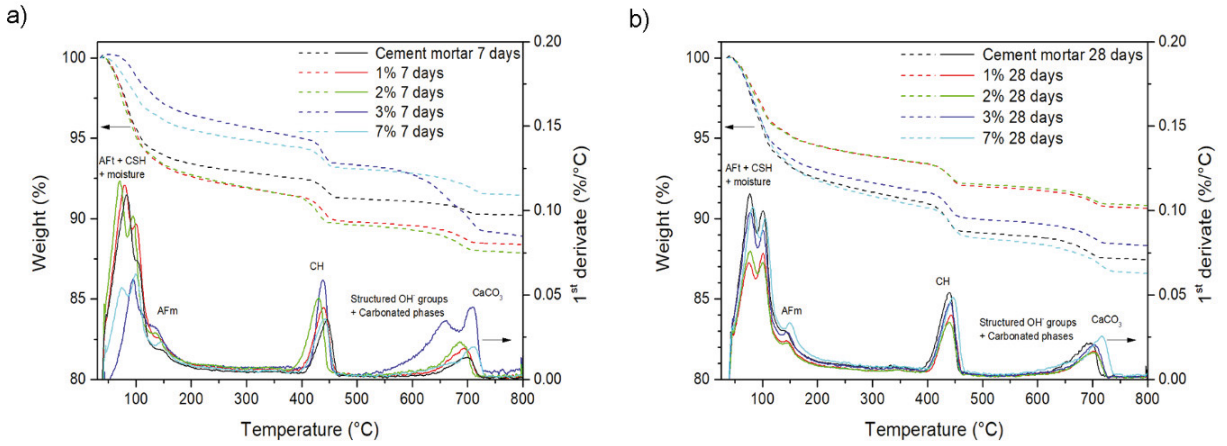


Fig. 5. Thermogravimetric Analysis of cement mortars specimens. (a) after 7 days of curing; (b) after 28 days of curing.

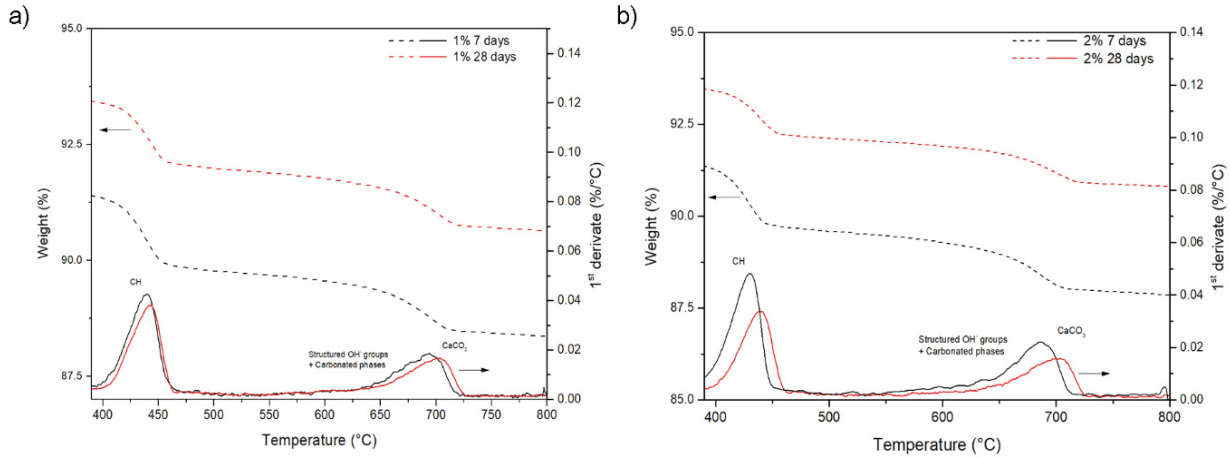


Fig. 6. TGA - DTA profiles of CH dehydration and carbonated decomposition of specimens containing. (a) 1% subtutition of nano $CaCO_3$; (b) 2% substutition of nano $CaCO_3$.

Figure 7 shows the CH content in cement mortars after curing for 7 and 28 days. After 7 days of curing, the specimens containing nano $CaCO_3$ have a higher CH content compared to simple cement mortars, which indicates the higher hydration rates at the early stages of curing. On the other hand, after 28 days of curing, the CH content is lower for specimens containing nano$CaCO_3$ which indicates a higher consumption through pozzolanic reaction to form more CSH and through further hydration of $C_4AF$ and CH to form $C_4AH_{13}$ and $C_4FH_{13}$. The further formation of CSH gel provides strength to the cement matrix, while the formation of $C_4AH_{13}$ and $C_4FH_{13}$ has no significant effects on the strength of hardened cementitious composites (Marangu et al. (2019)). However, these effects are less evident for a high $CaCO_3$ content (3 and 7%), which explains why compressive and flexural strength are higher in the specimen containing 2% substitution of nano $CaCO_3$ as seen in Figure 3.

XRD patterns in Figure 8 show crystalline phases present in the simple cement mortars and in the cement mortars with $CaCO_3$ nanoparticles after 7 and 28 days of curing. The spectra show the typical characteristics peaks for a cured cementitious matrix, i.e. the expected hydration products, including calcium hydroxide (portlandite), ettringite (AFt), poorly crystallized C–S–H and unreacted clinker phases (mainly calcium silicate phases). Calcite ($CaCO_3$) was not evident in the XRD analysis, unlike the TGA. This is probably due to the low content of calcite in the matrix. Alternatively, the calcite peak could overlap with the quartz peak at 2θ 29°. Quartz is the predominant crystalline phase in the specimens according to the high intensity of its peaks at 21 and 26°. The incorporation of $CaCO_3$ nanoparticles in the cement matrix enhances the hydration reaction, resulting in a higher amount of hydrated product

(CH and amorphous CSH) which is instead undetectable in the plane cement mortars. By increasing the amount of $CaCO_3$ in the cement matrix, the rate of hydration reaction increases. Specimens with 1% and 2% substutition of nano $CaCO_3$ exhibit a low quantity of hydrated products after 7 days, which is higher in specimens with 3% and 7% substutition of nano $CaCO_3$. XRD patterns of plane cement mortars after 28 days of curing show a change in the crystalline structure of the cement with respect to 7 days of curing, probably due to further pozzolanic reactions resulting in a high quantity of amorphous products (CSH). As already seen, after 7 days, specimens containing 7% of nano $CaCO_3$ exhibit higher flexural and compressive strength. This could be due to the higher content of hydrated compounds (CH) compared to the other specimens, which highlights the effect on the hydration rate of the cement during the early stages of curing. Instead, after 28 days of curing the specimens with the best performance were those containing 2% substutition of nano $CaCO_3$, which presented low content of dehydrated calcium silicates ($C_2S$ and $C_3S$) and also a low content of CH and quartz, thus highlighting the effect of pozzolanic reactions to form amorphous CSH.

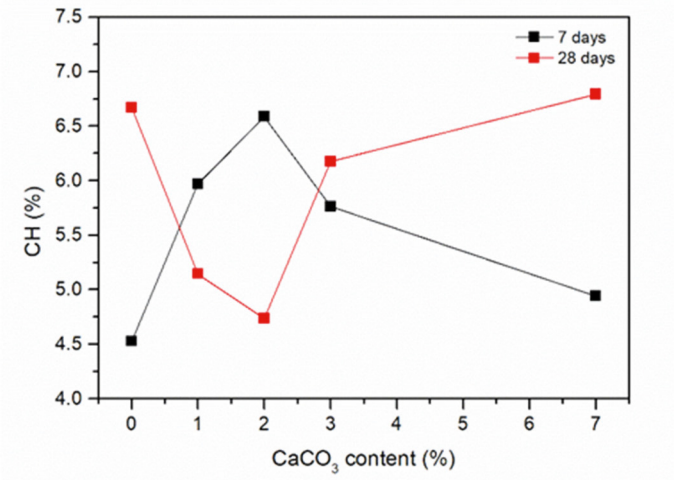


Fig. 7. Calcium hydroxide (CH) of plane specimens and specimens containing nano $CaCO_3$.

These findings suggest that there is a correlation between the cement hydration process and the resulting mechanical properties of cementitious composites. The incorporation of $CaCO_3$ nanoparticles in the cement matrix enhances the hydration reaction. In the early stages of curing, the flexural and compressive strength of the cement mortars improved with the content of nano $CaCO_3$. However, after 28 days of curing, percentages of substitution of nano $CaCO_3$ particles higher than 3% provided a lower improvement compared to the specimens containing 1 and 2% substitution of nano $CaCO_3$.

## 5. Conclusions

The present study investigates the effects of nano $CaCO_3$ particles on cement mortars, as they are additive materials with high potential for cementitious composites. $CaCO_3$ could be obtained from the $CO_2$ present in flue gases released during cement manufacturing. This study has shown that the incorporation of these nanoparticles provides a general improvement of the flexural strength in experimental specimens after curing for 7 and 28 days. Results from compression tests depend on the percentages of substitution of nano$CaCO_3$ used in the mixtures. The resulting trend was not uniform. Higher contents of nano $CaCO_3$ provided a smaller improvement of the mechanical properties of the cement mortars because of poor dispersion due to the agglomeration phenomena of the nanoparticles in the slurry and in the cement matrix. Research has also shown that nano $CaCO_3$ influences cement hydration, accelerating this process and increasing the early-age strength of cement mortars. Specimens containing 2% substitution of nano $CaCO_3$ exhibited the best performance highlighting the benefits of the nano $CaCO_3$ particles on the properties of the cement mortars. An important finding of this study is that the cement content can be decreased, thus reducing its carbon footprint. Recycling $CO_2$ could lead to the development of a circular economy approach in the cement industry. At the same

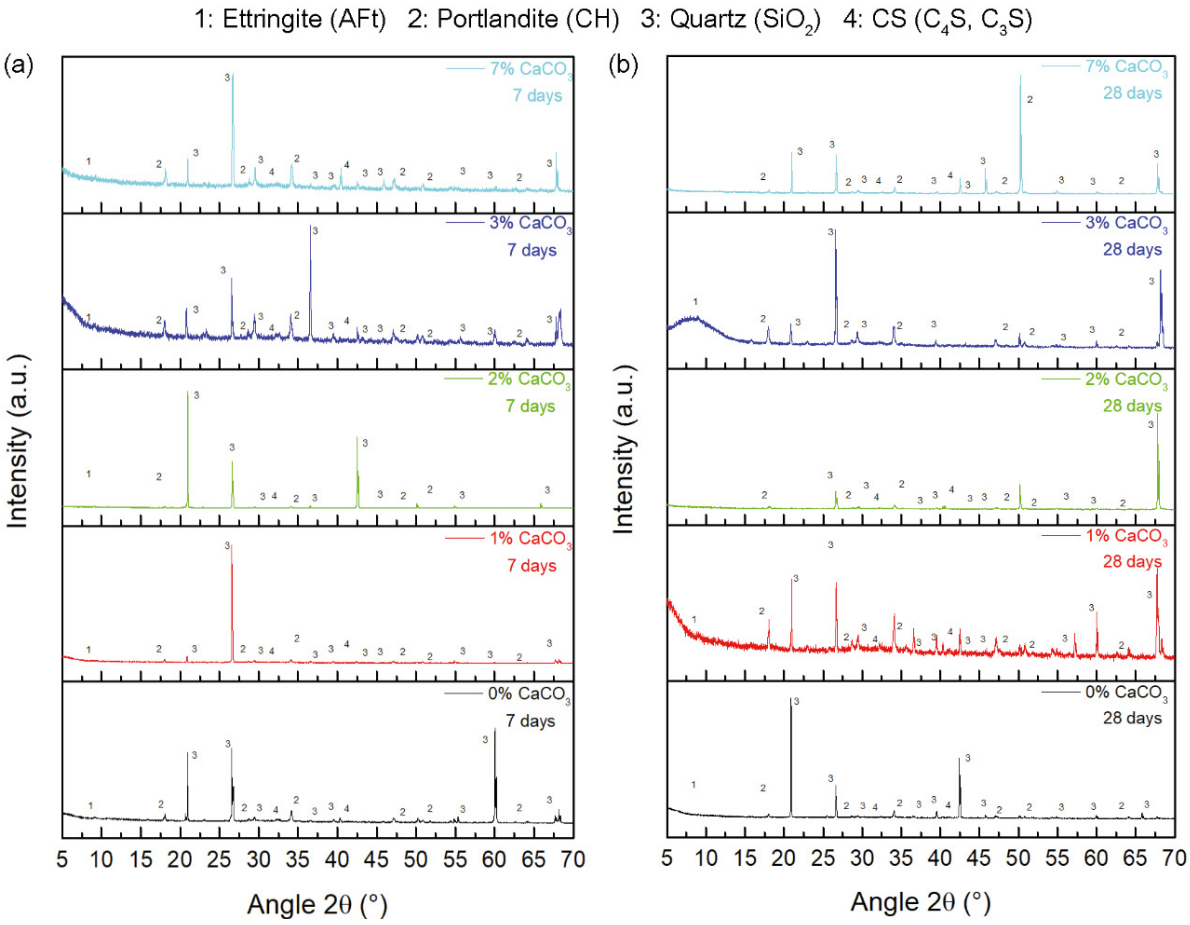


Fig. 8. XRD pattern of cement mortars specimens: (a) after 7 days of curing; (b) after 28 days of curing.

time, $CO_2$ could be used to produce valuable cement additives or concrete nanofillers, creating innovative and sustainable construction materials.

This study confirms the importance of nanotechnology in trasforming concrete technology. Obviously, these are preliminary results. Further mechanical tests are still needed to confirm these findings.

## Acknowledgements

This project has received funding from the European Union's Horizon 2020 research and innovation program under Grant Agreement number 768583 – RECODE (Recycling carbon dioxide in the cement industry to produce added-value additives: a step towards a $CO_2$ circular economy) project (https://www.recodeh2020.eu/).

## References

Andrew, RM., 2018. Global CO2 emissions from cement production. *Earth System Science Data* 10, 195–217.

Camiletti, J., Soliman, AM., Nehdi, ML., 2013. Effects of nano- and micro-limestone addition on early-age properties of ultra-high-performance concrete. *Materials and Structures/Materiaux et Constructions* 46, 881–898.

Camiletti, J., Soliman, AM., Nehdi, ML., 2013. Effect of nano-calcium carbonate on early-age properties of ultra-high-performance concrete. *Magazine of Concrete Research* 65, 297–307.

Cao, M., Ming, X., He, K., Li, L., Shen, S., 2019. Effect of macro-, micro- and nano-calcium carbonate on properties of cementitious composites-A review. *Materials* 12.

Chen, P-C., Tai, CY., Lee, KC., 1997. Morphology and growth rate of calcium carbonate crystals in a gas-liquid-solid reactive crystallizer.

*Chemical Engineering Science* 52, 4171–4177.
Cosentino, I., Ferro, GA., Restuccia, L., Bensaid, S., Deorsola, F., Liendo, F., 2019. Nearly zero CO 2 cementitious composites . *Material Design & Processing Communications*, 1–5.
Cosentino, I., Restuccia, L., Ferro, GA., Liendo, F., Deorsola, F., Bensaid, S., 2019. Evaluation of the mechanical properties of cements with fillers derived from the CO2 reduction of cement plants. *Procedia Structural Integrity* 18, 472–483.
Cosentino, I., Restuccia, L., Ferro, GA., Tulliani, JM., 2019. Type of materials, pyrolysis conditions, carbon content and size dimensions: The parameters that influence the mechanical properties of biochar cement-based composites. *Theoretical and Applied Fracture Mechanics* 103, 102261.
d'Amora, M., Liendo, F., Deorsola, FA., Bensaid, S., Giordani, S., 2020. Toxicological profile of calcium carbonate nanoparticles for industrial applications. *Colloids and Surfaces B: Biointerfaces*, 110947.
Daniyal, M., Akhtar, S., Azam, A., 2019. Effect of nano-TiO2 on the properties of cementitious composites under different exposure environments. *Journal of Materials Research and Technology* 8, 6158–6172.
Declet, A., Reyes, E., Suárez, OM., 2016. Calcium carbonate precipitation: A review of the carbonate crystallization process and applications in bioinspired composites. *Reviews on Advanced Materials Science*.
Ferro, G., Tulliani, JM., Lopez, A., Jagdale, P., 2015. New cementitious composite building material with enhanced toughness. *Theoretical and Applied Fracture Mechanics* 76, 67–74.
Ferro, GA., Ahmad, S., Khushnood, RA., Restuccia, L., Tulliani, JM., 2014. Improvements in self-consolidating cementitious composites by using micro carbonized aggregates. *Frattura ed Integrita Strutturale* 30, 75–83.
Gabrovšek, R., Vuk, T., Kaučič, V., 2006. Evaluation of the hydration of Portland cement containing various carbonates by means of thermal analysis. *Acta Chimica Slovenica* 53, 159–165.
H.F.W.Taylor., 1997. *Cement Chemistry 2nd Edition Chemistry for Engineers*.
Hashim, AM., Nhabah, HT., 2018. Influence of CACO3 with nanoparticles on the mechanical characteristics and concrete microstructure. *International Journal of Civil Engineering and Technology* 9, 799–808.
Kawano, J., Shimobayashi, N., Miyake, A., Kitamura, M., 2009. Precipitation diagram of calcium carbonate polymorphs: Its construction and significance. *Journal of Physics Condensed Matter* 21.
Khoshakhlagh, A., Nazari, A., Khalaj, G., 2012. Effects of Fe 2O 3 Nanoparticles on Water Permeability and Strength Assessments of High Strength Self-Compacting Concrete. *Journal of Materials Science and Technology* 28, 73–82.
Marangu, JM., Thiong'O, JK., Wachira, JM., 2019. Review of Carbonation Resistance in Hydrated Cement Based Materials. *Journal of Chemistry* 2019.
McDonald, L., Glasser, FP., Imbabi, MS., 2019. A new, carbon-negative precipitated calcium carbonate admixture (PCC-A) for low carbon Portland cements. *Materials* 12.
Nazari, A., Riahi, S., Riahi, S., Shamekhi, SF., Khademno, A., 2010. Influence of Al2O3 nanoparticles on the compressive strength and workability of blended concrete. *Jornal of American Science* 6, 6–9.
Restuccia, L., Ferro, GA., 2016. Promising low cost carbon-based materials to improve strength and toughness in cement composites. *Construction and Building Materials* 126, 1034–1043.
Restuccia, L., Ferro, GA., 2016. Nanoparticles from food waste: a "green" future for traditional building materials. .
Restuccia, L., Ferro, GA., 2018. Influence of filler size on the mechanical properties of cement-based composites. *Fatigue and Fracture of Engineering Materials and Structures* 41, 797–805.
Rodriguez-Blanco, JD., Shaw, S., Benning, LG., 2011. The kinetics and mechanisms of amorphous calcium carbonate (ACC) crystallization to calcite, via vaterite. *Nanoscale* 3, 265–271.
Sanchez, F., Sobolev, K., 2010. Nanotechnology in concrete - A review. *Construction and Building Materials* 24, 2060–2071.
Shaikh, FUA., Supit, SWM., 2014. Mechanical and durability properties of high volume fly ash (HVFA) concrete containing calcium carbonate (CaCO3) nanoparticles. *Construction and Building Materials* 70, 309–321.
Sobolev, K., Flores, I., Torres-Martinez, LM., Valdez, PL., Zarazua, E., Cuellar, EL., 2009. Engineering of SiO2 Nanoparticles for Optimal Performance in Nano Cement-Based Materials. *Nanotechnology in Construction 3*, 139–148.
Supit, SWM., Shaikh, FUA., 2014. Effect of Nano-CaCO3 on compressive strength development of high volume fly ash mortars and concretes. *Journal of Advanced Concrete Technology* 12, 178–186.
Zhou, GT., Yu, JC., Wang, XC., Zhang, LZ., 2004. Sonochemical synthesis of aragonite-type calcium carbonate with different morphologies. *New Journal of Chemistry* 28, 1027–1031.